# Period 3 regulates mitochondrial function via the NAD+-SIRT3 axis in mice

**Xiaoxian XIE**
Shanghai Jiao Tong University
**Ruonan Shu**
Zhejiang University of Technology
**Mengya Zhang**
Zhejiang University of Technology
**Donghong Cui**
Shanghai Jiao Tong University
**Lei Sun**
Zhejiang University of Technology
**Zezhi Li**
The Affiliated Brain Hospital of Guangzhou Medical University https://orcid.org/0000-0003-0241-1500
**Qi Han** ( qihan8@shsmu.edu.cn )
Indiana University School of Medicine

**Article**

**Keywords:** Per3, mitochondrial bioenergetics, NAD+-SIRT3 pathway, Nampt activity

**Posted Date:** July 5th, 2022

**DOI:** https://doi.org/10.21203/rs.3.rs-1767038/v1

# Abstract

Mitochondrial fission-fusion dynamics and bioenergetics are strongly clock-controlled. However, the mechanistic relationship between the clock and mitochondrial function remains largely unknown. Here we revealed that the clock gene *Per3* plays an essential role in the maintenance of mitochondrial homeostasis. Both *in vitro* and *in vivo* deletion of *Per3* consistently led to the disrupted mitochondrial integrity, including decreased mitochondrial membrane potential, impaired fission-fusion dynamics, increased oxidative stress, and altered mitochondrial bioenergetics. Mechanistically, we showed the binding of PER3 and BMAL1 to E-box regulatory elements in the promoter region of the nicotinamide phosphoribosyltransferase (*NAMPT*) gene promoted the gene activation as well as increased the NAMPT-dependent $NAD^+$ generation, which in turn induced the enzymatic activity of mitochondrial deacetylase SIRT3. Interestingly, administering nicotinamide mononucleotide (NAM), an $NAD^+$ precursor, protected cells from the *Per3* deletion-induced $NAD^+$ decline and associated mitochondrial dysfunction, whereas blocking of SIRT3's acetylation activity with 3-(1H-1, 2, 3-triazol-4-yl) pyridine abolished this beneficial effect of NAM on the global mitochondrial protein acetylation and homeostasis mechanisms. Collectively, we demonstrate that Per3 maintains mitochondrial integrity by regulating $NAD^+$-dependent SIRT3 activity and highlight a critical role for PER3 in mitochondrial homeostatic function.


# Introduction

Mitochondrial membranes are specially designed for aerobic respiration and produce the bulk of cellular ATPs by oxidative phosphorylation (OXPHOS) [1]. Recent evidence suggests that cellular energy metabolism and mitochondrial dynamics are rhythmically coordinated by the circadian clock [2, 3], which generates oscillations in the mitochondrial OXPHOS regulating the synthesis of nicotinamide adenine dinucleotide $(NAD)^+$ [4]. Studies have shown that disruption of the expression of circadian genes results in mitochondrial dysfunction [2, 4]. For example, deletion of *Bmal1*, a principal driver of the molecular clock in mammals, in the liver impairs the mitochondrial $NAD^+$ turnover and alters the expression of genes related to rhythmic mitochondrial dynamics, thus resulting in the mitochondrial dysfunction [4, 5].

The cellular $NAD^+$, as a redox carrier, is essential for the completion of diverse metabolic processes such as glycolysis, fatty acid oxidation (FAO), amino acid degradation, and the tricarboxylic acid (TCA) cycle. $NAD^+$ serves as a critical co-substrate for $NAD^+$-consuming enzymes, including sirtuins (SIRTs), poly (ADP-ribose) polymerases, and cyclic ADP-ribose hydrolase (CD38) [6]. The age-associated decline of the $NAD^+$ level regulates the activity of SIRT3 in the mitochondria, leading to mitochondrial damage [7, 8]. Strategies to boost $NAD^+$ synthesis via administration of $NAD^+$ precursors have shown promising treatment effects in rodents of different disease models, including noise-induced hearing loss [9], high-fat diet-induced obesity [10], and heart failure [11]. In addition, $NAD^+$ synthesis boosts postpartum functions in mice [12], suggesting the importance of maternal supplements on human health. Although several mechanisms have been reported to potentially modulate $NAD^+$ availability in cells, it remains unclear how

$NAD^+$ salvage capacity is regulated by mitochondrial function and whether disturbances in circadian and behavior-related genes control the cellular $NAD^+$ level.

Three period (*PER*) genes, *PER1, PER2*, and *PER3*, have been identified as the major component of the circadian clock where there play differential functions in the clock regulation [13]. PER1/2 proteins play a role in the demand-based optimization of mitochondrial metabolism to balance the daily energy production/expenditure [2, 3]. In mice, dual knockout (KO) of Per1/2 alters the daily oscillations in levels of rate-limiting mitochondrial enzymes, such as CPT1 and PDH, and proteins involved in the OXPHOS. Despite Per3's role in the cellular circadian clock maintenance [14], our understanding of the mechanistic impact of Per3 functional perturbation in mitochondria and cellular $NAD^+$ metabolism remains limited.

In this study, we demonstrated that deletion of *PER3* either *in vitro* or *in vivo* dramatically affected mitochondrial biology, including improper maintenance of the membrane potential, alterations in the fission-fusion dynamics, and a reduction in cellular energy production. We further revealed that PER3 regulated mitochondrial homeostasis by altering the $NAD^+$-SIRT3 axis. PER3 was found to form a complex with BMAL1, which bound E-Box sequences to control the expression of the nicotinamide phosphoribosyltransferase (*NAMPT*) gene. Inhibition of PER3 activity decreased the cellular $NAD^+$ level, thereby, diminishing SIRT3 activity. Exogenous administration of nicotinamide (NAM), a NAD precursor, could partially restore the *PER3*-deletion-induced mitochondrial dysfunction by reactivating the $NAD^+$-SIRT3 axis.

## Results

# Loss of PER3 affects the cellular energy balance in liver

To examine whether *PER3* deletion affects cellular transcriptome, we carried out RNA sequencing (RNA-seq) analysis from the liver samples of both wild type (WT) and *Per3* KO mice at the age of 7 months. The first principal component (PC1) analysis of transcription profiles demonstrated the variation between the liver expression profiles of WT mice from that of the *Per3* KO mice (Fig. 1A). The Volcano plot of RNA-seq transcriptome data of two groups identified significant (false discovery rate [FDR] $P \leq 0.05$) differential expressions of 658 genes, including 445 upregulated and 213 downregulated genes (Fig. 1B, C). Gene ontology (GO) analysis of the remaining differentially expressed genes (DEGs) revealed that Per3 regulated DEGs that were mainly involved in the energy production and conversion, suggesting Per3's possible role in cellular energy homeostasis (Fig. 1D). To gain a better understanding of the PER3-mediated signaling pathways that might be involved in the bioenergetic transcriptional programming, we performed the Kyoto Encyclopedia of Genes and Genomes (KEGG) pathway analysis and observed enrichment of previously reported signaling factors related to the energy metabolism pathways [15], as well as the OXPHOS and glutathione metabolism pathways (Fig. 1E). Together, these data suggest that PER3 may simultaneously control multiple signaling pathways that are involved in the cellular bioenergetics.

# Loss of PER3 disrupts mitochondrial homeostasis and energy metabolism

Given that the cellular bioenergetic mechanisms are tightly controlled by mitochondria, we hypothesized that mitochondria might undergo structural and/or functional changes in the liver of *Per3* KO mice. First, we examined the rate of mitochondrial fragmentation in the adult mice liver tissue by using a transmission electron microscope (TEM) and found that WT mice liver cells had normally fused mitochondria, while the *Per3* KO mice hepatic cells contained intermediate-sized and fragmented mitochondria (Fig. 2A). To explore the upstream mechanism, we examined the expression of Drp1 and mitochondria fusion factors mitofusin 1 and 2 (Mfn1/2). We found that *Per3* KO mice livers had high expression of Drp1 mRNA, but low expressions for Mfn1 and Mfn2 compared with that of WT mice (Fig. 2B). Since mitochondrial fragmentation is critical for the activation of mitophagy [16], we further investigated the status of PTEN-induced putative kinase 1 (PINK1)-PARKIN-dependent mitophagy in our mice model. As expected, *Per3* KO hepatic cells exhibited a reduced level of Parkin expression than in WT mice cells (Fig. 2C, D), indicating Parkin-mediated mitophagy may be inhibited in response to the Per3 depletion-induced disruption of mitochondrial integrity in liver cells. Measurement of mitochondrial membrane potential serves as a potential indicator of the functionality of the mitochondrial electron transport chain (ETC) system [17]. In this assay, shifts from red to green fluorescence were recorded in 2.76% of WT primary mouse embryonic fibroblasts (PMEFs) compared to that of 10.2% in Per3 deficient PMEFs (Fig. 2E). These data collectively suggest that Per3 deficiency may lead to the loss of mitochondrial membrane potential.

# Loss of PER3 induces oxidative stress in liver cells

Since mitochondrial dysfunction is associated with increased reactive oxygen species (ROS) production, we assessed the impact of *Per3* deletion on ROS generation and the cellular redox state. We measured the cellular ROS level by mitochondrial superoxide indicator, MitoSOX Red, and then determined the population of cells with measurable ROS levels by flow cytometric analysis. Consistently, we found a significantly high level of ROS production in *Per3* KO but not in WT PMEFs (Fig. 3A). To test whether mitochondrial dysfunction can modulate the ETC redox status, we examined the expression of glutathione (GSH) and other redox enzymes, which revealed diminished GSH levels in liver cells of *Per3* KO mice compared with that in WT mice (Fig. 3B). The qRT-PCR quantification of redox proteins' mRNA levels also showed decreased expressions of antioxidant genes, including superoxide dismutase 1 (*SOD1*), *SOD2*, glutathione S-reductase (*GSR*), and glutathione peroxidase (*GPx)* (Fig. 3C). Taken together, these data revealed that loss of *Per3* in liver cells increased ROS-mediated oxidative stress, resulting in mitochondrial dysfunction.

# PER3 regulates mitochondrial homeostasis via the $NAD^+$-SIRT3 axis

Circadian genes have been well studied in the context of metabolic regulation. Hence, we hypothesized that Per3 might regulate the intracellular $NAD^+$ level. The ELISA assay exhibited that the Per3 loss could reduce the physiological level of $NAD^+$ in the liver of *Per3* KO mice in comparison to controls (Fig. 4A). Since NAMPT plays a predominant role in the $NAD^+$ biosynthesis [18, 19], we tested the enxpression and activity of Nampt i *Per3* KO vs. WT mice and found a > 50% of reduction in Nampt activity compared to that in the WT mice (Fig. 4B). Western blotting also revealed significantly decreased Nampt protein levels in *Per3* KO mice (Fig. 4C).

Because $NAD^+$ serves as a cofactor for mitochondrial SIRTs that regulate mitochondrial protein acetylation [20, 21], we speculated that Sirt3 function might alter due to Per3 depletion in *Per3* KO mice. Immunoblotting and qRT-PCR analysis showed that neither Sirt3 mRNA nor its protein expression was affected by Per3 depletion in the liver cells of *Per3* KO mice compared to WT mice liver cells (Fig. 4D, E). Interestingly, the enzymatic activity of SIRT3 was negatively impacted by Per3 loss in liver cells of *Per3* KO mice (Fig. 4F), indicating that PER3 is indispensable for SIRT3's enzymatic activity, possibly via $NAD^+$ utilization. SIRTs can act as metabolic sensors that adjust cellular metabolism rate according to the metabolic need of the body, which provoked us further to investigate the ATP contents of liver cells with *Per3* deletion. As expected, we found the decreased activity of ATP synthase, leading to a relatively low yield of ATP in *Per3* KO mice (Fig. 4G, H).

Next, we validated whether the $NAD^+$-SIRT3 signaling pathway was required for PER3 deletion-induced mitochondrial dysfunction. Nicotinamide (NAM)-treated *Per3* deleted liver cells were able to rescue the protein level of Mfn1, which was abolished by blocking the SIRT3 enzyme with 3-(1H-1,2,3-triazol-4-yl) pyridine (3-TYP) (Fig. 4I-L). Whereas, no change was observed in Mfn2 and Drp1 levels. Notably, inhibition of SIRT3 enzyme activity also reduced the production of ATP in *Per3*-deleted liver cells that were treated by NAM (Fig. 4M; **Fig. S1A**). Furthermore, we found that incubation of *Per3* KO cells with honokiol, an activator of SIRT3 [22], could rescue the mitochondrial dysfunction, especially by increasing the level of ATP production, coupled with an elevated level of Mfn1 (Fig. 4N-Q; **Fig. S1B-C**), suggesting that PER3 may be an essential regulator of SIRT3's enzymatic activity and mitochondrial functionality, as well, primarily through the cellular ATP synthesis. Altogether, these observations suggest that the clock gene *PER3* product may modulate mitochondrial homeostasis and bioenergetics via the $NAD^+$-SIRT3 axis in the liver cells.

# Transactivation by PER3-BMAL1 heterodimers from Nampt E-boxes

In mammalian cells, the NAM salvage pathway is recognized as the principal contributor to $NAD^+$ synthesis. $NAD^+$ is involved in the sequential actions of NAMPT and nicotinamide nucleotide (NAMN) adenylyltransferases 1–3 (NMNAT1-3). NAMPT forms NAMN and pyrophosphate (pp) from NAM that is generated by SIRTs, Poly(ADP-ribose) polymerases (PARPs), and α-D-5-phosphoribosyl-1-pyrophosphate (α-PRPP). On the other hand, NMNAT1-3 produces $NAD^+$ from NAMN and ATP [18, 19]. However, whether

the clock-controlled PER3 binds to E-boxes of NAMPT regulating its expressioatn requires further investigion. To do this, we screened DNA sequences of the *NAMPT* gene and its proximal regions that might allow direct interactions. Through bioinformatics analysis, we identified two DNA sequences of putative E-boxes within the *Nampt* gene that were highly conserved in mice [19]. One of the sites was located within 488-454bp (E-box1) of intron1, downstream of the transcriptional start site (TSS), while the other one (E-box2) was located in the 902–916 bp region of intron 9. Thus, we investigated whether these sites were correlated with the Per3-mediated activation of *the Nampt* gene.

We, therefore, constructed two luciferase reporters containing E-box1, and E-box2 sequences, respectively. We then ectopically co-expressed PER3 and luciferase reporter in HEK293T cells. The E-box1 transfected cells showed higher luciferase activity compared to that of E-box2 cells, following the PER3 overexpression (Fig. 5A-B). To determine the role of E-box1 in driving NAMPT activity, we introduced point mutation in the canonical E-box1 sequence, which abolished the enzymatic activity of NAMPT (Fig. 5A), suggesting that E-box1 plays a stronger role in NAMPT's transcriptional activity than its counterpart E-box2. An immunoblotting experiment using an anti-NAMPT antibody revealed that PER3 overexpression could restore the NAMPT activity to a comparable level with WT cells, where the E-box1 motif plays a key regulatory role in modulating the enzymatic activity (Fig. 5C-D).

It is now well-established that PER proteins regulate the circadian rhythm by interacting with the transcriptional-translational feedback loop of clock proteins. BMAL1 is a core clock element that drives the transcription of *PER* and *Cryptochrome (CRY)* genes by binding their E-box elements [23]. Therefore, we investigated whether PER3 would associate with BMAL1 to regulate the transcriptional activity of the CLOCK-BMAL1 axis in a transcriptional-translational feedback manner. To verify this, we performed a co-immunoprecipitation (co-IP) assay to pulldown PER3 using an anti-FLAG antibody from FLAG-HA-tagged BMAL1 fusion protein-expressing mouse liver cell extracts. This assay revealed PER3 as one of the interacting partners of the BMAL1 complex. We further confirmed this interaction by reverse co-IP using an anti-PER3 antibody from mouse liver cell extracts (Fig. 5E). In summary, PER3 is a constituent of the endogenous BMAL1 complex. To further determine the interaction between PER3 and E-box1 sequence, we performed a chromatin immunoprecipitation (ChIP) assay from WT and *Per3* KO cells. We found that immunoprecipitation PER3 led to the coprecipitation of BMAL1 at E-box1 site relative to the immunoprecipitation of the same region with control IgG antibodies in total protein from WT cells, but Per3 KO abolished this effect (Fig. 5F). Similarly, immunoprecipitation BMAL1 led to the coprecipitation of PER3 at E-box1 site (Fig. 5G), suggesting that BMAL1 and PER3 bind the E-box1 element to regulate the expression of *NAMPT*.

# NAM mitigates PER3 deletion-induced mitochondrial energy stress

NAM is largely made available for the $NAD^+$ salvage via degradation of dietary $NAD^+$ and NADP, and it is considered one of three $NAD^+$ precursor vitamins. Next, we investigated whether chronic NAM supplementation would improve the regeneration of cytosolic $NAD^+$ in the liver of *Per3* KO mice. After oral

supplementation of NAM to WT and *Per3* KO animals for 12 weeks, we found that the KO mice had increased levels of $NAD^+$ in the liver, comparable to that of WT mice(Fig. 6A; **Fig. S2A**). Notably, the abundance of NAMPT, which catalyzes the conversion of NAM into NAMN, was also significantly higher in *Per3* KO mice following the NAM administration compared with *Per3* KO sham controls (Fig. 6B, C; **Fig. S2B**). Taken together, these findings showed that NAM supplementation increased the activity of SIRT3 and ATP synthase (Fig. 6D, E; **Fig. S2C, D**) and ATP content in Per3 deficient mice from 10–15% o that in the liver of WT mice (Fig. 6F; **Fig. S2E**).

Next, we interrogated the activity of the $NAD^+$-SIRT3 pathway *in vitro* to further assess the impact of NAM on energy metabolism. We isolated PMEFs from *Per3* deficient mice at the age of eight weeks. We found supplementation of NAM in *Per3 KO* PMEFs significantly promoted the activity of both SIRT3 and ATP synthase, companied by an increase in $NAD^+$ level, which returned to the baseline value of WT PMEFs (Fig. 6F, G; **Fig. S2F-H**). Instead, blocking SIRT3 activity with 3-TYP prevented NAM supplementation-induced energy restoration in *Per3* KO PMEFs (Fig. 6G-I; Fig. 4M). Cumulatively, these results suggest that NAM supplementation can rescue PER3 depletion, along with the reversal of cellular energy stress in the liver in a SIRT3-dependent manner.

# Discussion

Circadian clock gene *PER3* is reported to have a prominent role in the adipocyte precursor cell clock, especially mediating the Klf15-associated adipogenesis [24]. *PER3* can also form a complex with peroxisome proliferator-activated receptor γ (PPARγ) to modulate adipogenesis via inhibiting its transcriptional activation [25]. Interestingly, a recent study has shown that *Per3* knockout mice display depression-like behaviors, which increased significantly during exposure to a short photoperiod [26]. However, the function of the *PER3* gene in the regulation of mammalian physiology is still poorly understood. In this study, we showed that PER3 is essential for mitochondrial homeostasis, and the deletion of PER3 in liver cells altered the activity of the NAMPT-$NAD^+$-SIRT3 axis, leading to a decline in $NAD^+$ level and mitochondrial dysfunction.

Mitochondrial fusion-fission dynamics is a critical quality control mechanism to ensure mitochondrial integrity and energy bioenergetics [27]. Mitochondrial fusion is modulated by different proteins, including MFN1, MFN2, and OPA1 [28]; while mitochondrial fission is mediated mainly by DRP1 [29]. In this study, we found that *Per3* KO liver cells displayed reduced levels of both Mfn1 and 2 but increased Drp1 levels, suggesting that PER3 could modulate the balance of the mitochondrial fusion-fission process. Besides, we observed that *PER3* deletion caused improper maintenance of mitochondrial membrane potential, abnormal cristae structures, and insufficient ATP production in mice liver cells. These results suggest that loss of Per3 in liver cells could disrupt the overall mitochondrial integrity.

The cumulative oxidative stress is considered a major etiological factor for numerous human diseases, and this stress results from the production of ROS [7]. The mitochondrial free radical theory of aging hypothesizes that the ROS-induced oxidative stress originates from disturbances in the mitochondrial

respiratory chain [30]. Consistent with this hypothesis, mitochondria are a major source of cellular ROS and thus, ROS-induced oxidative damage, which leads to the declined mitochondrial function [31]. Here, the increased ROS content was detected in Per3 deficient mice, suggesting that the elevated oxidative stress may result from Per3 depletion. ROS are scavenged by antioxidant enzymes that help maintain a reducing environment in the mammalian cells. An imbalance between the production of ROS and the ability of cells to readily detoxify that ROS impairs the reducing environment, leading to the oxidative stress [30, 32]. These data demonstrate that significantly reduced expression of genes, encoding antioxidant enzymes, was accompanied by elevated ROS production. Overall, Per3 deficiency in mice results in an imbalance in the oxidative stress production/utilization, which may impact the mitochondrial function.

In mammalian cells, the principal contributor to $NAD^+$ synthesis is the NAM salvage pathway that involves sequential actions of NAMPT and NMNAT1-3 [18]. We found that the activity of NAMPT was significantly reduced in the liver of *Per3* KO mice, suggesting decreased synthesis of $NAD^+$ might be due to the down-regulation of NAMPT reaction. The previous study shows that the lack of clock gene *BMAL1* in the liver reduced the activity of SIRT3 and elevated mitochondrial protein acetylation, causing the dysfunction of oxidative enzymes [29]. Likewise, we demonstrated that the reduced activities of SIRT3 and ATP synthase were detected in the liver of *Per3* KO mice in comparison to wild-type mice. However, there was no significant difference in Sirt3 mRNA and protein expressions between *Per3* KO and WT mice, suggesting that loss of PER3 could affect SIRT3 deacetylase activity rather than its transcription or translation in the liver. Our subsequent experiments further confirmed that the PER3-induced alterations of SIRT3 enzyme activity are attributed to the changes in $NAD^+$ concentrations, which were regulated by NAMPT. The NAMPT-$NAD^+$-SIRT3 axis is essential for maintaining mitochondrial integrity and homeostasis in the liver cell with the *Per3* deletion [9, 33]. Although NAM administration could be protective against mitochondrial dysfunction by increasing $NAD^+$ availability, however, Sirt3 ablation could compromise such effect in *Per3* KO mice. In terms of cellular energetics, we realized that the metabolic behavior of PER3 deletion-induced energy stress was also consistently observed in liver cells from mice with *Per1/2* deletions [13]. Taken together, our results demonstrate that PER3 plays a critical role in mediating mitochondrial homeostasis through the $NAD^+$-SIRT3 axis under normal physiological conditions.

Previous studies have shown that there are canonical or non-canonical E-box motifs in the promoter and first intron of the *NAMPT* gene [18, 19]. In combination with bioinformatics analysis and co-IP assay, we reveal that PER3 bind the canonical E-box in the first intron of the *NAMPT* gene, but not the other three non-canonical E-boxes in the promoter region. Transduction or knockdown of Per3 in the mouse PMEF appeared to either upregulate or downregulate the Nampt expression, suggesting that Per3 might directly regulate NAMPT-mediated $NAD^+$ biosynthesis. Particularly, we identified that PER3 and BMAL1 form a complex to execute this function, which was consistent with a previous study showing PER proteins can form a complex with other clock components [24]. Hence, these data demonstrate that PER3 can directly regulate NAMPT expression in complex with BMAL1 bound to the canonical E-box.

As a cofactor for several enzymes, $NAD^+$ is fundamental to the cellular bioenergetic metabolisms [34, 35]. A reduction in $NAD^+$ levels leads to mitochondrial dysfunction and metabolic abnormalities. Recent studies have identified that supplementation with $NAD^+$ precursors, including NAMN [36], NR [12], and NAM [37], inhibiting the activity of $NAD^+$-consuming enzymes can increase the $NAD^+$ level and improve the overall energy metabolism [8], thereby delaying aging and extending healthy life. These reports support our observations that NAM administration in Per3 deficient mice for 12 weeks can elevate the level of $NAD^+$. The increased $NAD^+$ level has a strong metabolic impact because it acts as a cofactor for SIRTs, including SIRT3, a histone deacetylase that regulates a wide range of mitochondrial proteins [38]. Additionally, elevated NAMPT activity was detected in *Per3* KO mice, which was consistent with the previous observations that boosting $NAD^+$ levels by the administration of NAD precursors could activate the NAMPT [39]. In our study, supplementing with NAM ameliorated the mitochondrial dysfunction and restored the capacity of ATP generations in *Per3* KO mice. Once again, such effect of NAM-mediated mitochondrial/ATP restoration is mainly dependent on the NAMPT/$NAD^+$-SIRT3 driven pathway in *Per3* KO mice. Furthermore, the loss of SIRT3 could reverse this effect by altering mitochondrial protein acetylome and probably by remolding metabolic coupling between fuel-producing and fuel-consuming tissues [38–41].

In conclusion, our study reveals that the circadian gene, *PER3*, maintains mitochondrial function through the NAMPT/$NAD^+$-SIRT3 driven pathway, which functions to regulate the cellular energetic and oxidative metabolism, as well as serve as a potential therapeutic target for mitochondria-related diseases.

## Materials And Methods

# Animals

Six-week-old C57BL/6J mice were purchased from China National Laboratory Animal Research Center (Shanghai Shilaike Co., Ltd., China). For experiments using *Per3* KO mice, male and female *Per3* KO mice were purchased from the Model Animal Research Center and the Medical School of Nanjing University (Nanjing, China). These mice were developed from embryonic stem cells (ESCs) with a retroviral promoter trap that functionally deletes one allele of the *Per3* gene, and *Per3* KO mice have backcrossed at least six generations onto C57BL/6J background. *Per3* KO mice were cross-fertilized to derive a required number of experimental animals. Control and *Per3* KO mice received standard chow and water *ad libitum*. Animals at their 7 months of age were anesthetized with 100μl of Nembutal before tissue collection. All experiments were performed in accordance with protocols approved by the Animal Care Facility and Use Committee of Zhejiang University of Technology (Hangzhou, China).

# Plasmid DNA construction

Mouse *Per3* cDNA was sequenced and compared with the National Center for Biological Information (NCBI) reference sequence for the mRNA of *Per3*. Mouse *Per3* was then PCR amplified using their cDNA as a template and then cloned into a pcDNA3.1/myc-His (–) vector (Invitrogen, Carlsbad, CA, USA).

# Cell culture and enzyme activity assay

PMEFs were isolated from WT and *Per3* KO mice as previously described by [42], and the primary hepatocytes were isolated as described elsewhere [43]. Then, cells were cultured in 6-well plates containing 5mL of Dulbecco modified Eagle medium (DMEM; Gibco) supplemented with 10% fetal calf serum, and the medium was changed every 3 days. Once cells reached 85–90% confluency, they were passaged for sub-culturing.

For activation or inhibition of the SIRT3 enzyme, cells were incubated in 10μM of SIRT3-specific activator honokiol (Selleck Chemicals, USA) solution prepared in incubation buffer, or were incubated in a 50μM of SIRT3-selective inhibitor 3-TYP (MedChemExpress, Shanghai, China). The activity of SIRT3 (Abcam, Cambridge, MA, USA) and NAMPT (Abcam) were measured using Enzyme Activity Assay Kit, and the ATP synthase was analyzed using Enzyme Activity Microplate Assay Kit (Abcam), according to the manufacturer's protocol.

# Real-time quantitative PCR (qRT-PCR)

Fresh liver tissues were harvested, and total RNA was extracted using the TRIzol reagent (Invitrogen). Total RNA was directly amplified with the QuantiTect SYBR Green RT-PCR kit (Toyobo, Tokyo, Japan). The amplified levels of selected genes were then calculated using GAPDH as an internal standard. Specific primers used in this experiment are listed in **Supplemental Table 1**.

# Antibodies and western blot analysis

For whole-cell extracts, PMEFs and their modified ones were homogenized in RIPA buffer (20mM Hepes pH 7.5, 100μM sodium orthovanadate, 100mM KCl, 0.1% Triton X-100, 20mM β-glycerophosphate, 1mM DTT, 10mM EDTA, 5% (v/v) glycerol, 1% protease inhibitor mixture (Roche), and 1% phosphatase inhibitor mixture (Active Motif)). Mouse livers were homogenized in extraction buffer (20mM Hepes pH 7.5, 100μM sodium orthovanadate, 100mM KCl, 0.1% Triton X-100, 20mM β-glycerophosphate, 1mM DTT, 10mM EDTA, and 5% (v/v) glycerol) containing protease inhibitor mixture (Roche), and phosphatase inhibitor mixture (Active Motif). After centrifugation, the supernatants were boiled for 10min in the SDS sample buffer and then separated by running on the SDS/PAGE. After transferring to PVDF membranes (Immobilon FL, Millipore EMD), the membrane blocking was performed with BSA containing blocking buffer. Protein expression was detected with the following antibodies: mouse anti-LC3 (Abcam, Burlingame, CA, USA), anti-SIRT3 (Cell Signaling Technology, Beverly, MA, USA), mouse anti-MFN1 (Abcam, Burlingame, CA, USA), 1:1,000; mouse anti-MFN2 (Abcam), 1:1,000; anti-DRP1 (Abcam), 1:1,000; anti-Nampt (Abcam), 1:1,000; and anti-β-actin (1:5,000), purchased from Cell Signaling Technology, and was served as a loading control and for normalization.

### NAD $^{+}$ and ATP quantification from mouse liver and cel/

For the $NAD^{+}$ assay, a pellet of $2\times10^{5}$ cells or 20mg of liver tissue for each assay was extracted with 400μL of NAD extraction buffer by homogenization or freeze/thawing for 2 cycles of 20min. After

proteinase treatment, 50μL of extracted samples in duplicate were placed into 96-well plates, and 100μL of the master reaction mix was added and incubated for 5min at room temperature to convert $NAD^+$ to NADH. These reaction mixtures were mixed with 10μL of NADH developer and incubated for 1-4h. The time was dependent on color development, which was measured at 450nm absorbance. The amount of NAD present in the samples was determined from the standard curve.

For ATP assay, primary hepatocytes were plated in 6-well plates and grown to 80% confluency. The cell culture media was removed, and fresh media containing galactose (4.5g/liter) was added and incubated for 24h. The cells and liver sections were homogenized in 50% of aqueous high-performance liquid chromatography (HPLC) grade acetonitrile containing 0.3% formic acid, frozen in liquid nitrogen for tandem mass spectrometry. After hepatic protein precipitation with methanol, the supernatants were dried and esterified with hot, acidic methanol. Then, the ATP content of cell and liver samples was measured using HPLC and normalized to protein content.

# Construction of plasmid and vectors

E-box 1 and 2 of the first intron of the *NAMPT* gene were subcloned into the Pgl4 luciferase reporter vector (Promega, Madison, WI, USA). A full-length cDNA fragment of *Per3* was sub-cloned in a pEF6/V5-His expression plasmid (Invitrogen, Carlsbad, CA, USA). The site-directed mutagenesis was performed using the Quick Change site Directed Mutagenesis kit following the protocols of the manufacturer (Stratagene, La Jolla, CA, USA).

# Transient transfections and reporter assays

The reporter plasmids were co-transfected into HEK293T cells with expression plasmids containing the full-length cDNA of *Per3* and *Bmal1* or control plasmids in 24-well plates using Lipofectamine 3000 (Invitrogen). Then, the luciferase assays were carried out by using Luciferase Assay kits (Promega, Madison, WI, USA) following the descriptions as the manufacturer's protocol.

# Chromatin immunoprecipitation (ChIP) assay

ChIP assay was carried out using a simple ChIP Plus Enzymatic Chromatin IP Kit (Cell Signaling Technology, Beverly, MA, USA), following the manufacturer's instructions. Briefly, PMEFs were cross-linked in 1% formaldehyde for 10min at room temperature. After the cross-linking, cells were washed with pre-chilled PBS, followed by digestion with micrococcal nuclease for 20min. The supernatant was collected, and immunoprecipitation was carried out using anti-PER3 (Abcam, Cambridge, UK) and anti-BMAL1 (Abcam, Cambridge, UK) antibodies or normal IgG. Samples were incubated with protein A/G agarose/Sepharose that precipitated endogenous DNA-protein complexes. Then, the cross-linking was reversed. Finally, proteinase K was added to the reaction mix to recover DNA fragments. The qPCR was performed to quantify the amount of precipitated DNA bound to the target protein. The specific primers are listed as follows: E-box1 forward, 5′- AACTCGAGTAGGTAACAGCCCCTGGCT − 3′; reverse, 5′-AAAAGCTTTTAAAGCAATGTGCCATTTTACTC − 3′), and control site (forward, 5′-

AACTCGAGATACTTCAGATACTTTAAGTCATTCTGT − 3′; reverse, 5′-AAAAGCTTACAGATGTGTTTGCAAACTACAGA − 3′).

Immunoprecipitation (IP) was carried out using the nuclear complex IP kit, as per the manufacturer's instructions. The SDS-PAGE fractionation and immunoblot assay were performed using anti-BMAL1 (Abcam) or PER3 (Abcam) antibodies.

# Statistical analysis

Data were presented as mean ± S.E.M. Statistical analyses comparing two parameters were conducted using a two-tailed student's *t*-test. Two-parameter analyses for samples of *in vivo* studies were performed using the Mann-Whitney test and one-way analysis of variance (ANOVA) followed by the Bonferroni post hoc test for multiparameter analyses. $*p < 0.05$ was considered statistically significant.

# Declarations


## ACKNOWLEDGEMENTS

The authors express their gratitude to STEVEN M. REPPERT, and David R. Weaver, Ph.D. (Professor, Department of Neurobiology, program in Neuroscience; University of Massachusetts Medical School) for their great input in our article.


## AUTHOR CONTRIBUTIONS

All authors contributed to this work. Qi Han, Xiaoxian Xie and Zezhi Li conceived and designed the article, and checked the quality of writing, and revised the article critically for important intellectual content; Xiaoxian Xie and Rongnan Shu mainly performed the experiments and additional Qi Han drafted the article; Chunan Yu, Mengya Zhang and Lei Sun involved in performing the experiments and made the statistical analysis; Donghong Cui conceived our article.


## FUNDING

This work was supported by grants from Zhejiang Provincial Natural Science Foundation of China (No. LY20C110002), the National Natural Science Foundation of China (No. 31701028). All funding had no role in study design, data analysis, paper submission and publication.


## COMPETING INTERESTS

The authors declare no competing interests.

## ETHICS STATEMENT

All experiments were performed in accordance with protocols approved by the Animal Care Facility and Use Committee of Zhejiang University of Technology (Hangzhou, China).

### AVAILABILITY OF DATA AND MATERIALS

The datasets used and analyzed during the current study are available from the corresponding author on reasonable request.

# References


1. Ezagouri S, Asher G. Circadian control of mitochondrial dynamics and functions.Curr Opin Physiol. 2018;5(1):25–29.
2. de Goede P, Wefers J, Brombacher EC, Schrauwen P, Kalsbeek A. Circadian rhythms in mitochondrial respiration.J Mol Endocrinol. 2018;60(3):115–130.
3. Neufeld-Cohen A, Robles MS, Aviram R, Manella G, Adamovich Y, Ladeuix B, et al. Circadian control of oscillations in mitochondrial rate-limiting enzymes and nutrient utilization by PERIOD proteins.Proc Natl Acad Sci USA. 2016;113(12):1673–1682.
4. Peek CB, Affinati AH, Ramsey KM, Kuo HY, Yu W, Sena LA, et al. Circadian clock $NAD^+$ cycle drives mitochondrial oxidative metabolism in mice. Science. 2013;342(6158):1243417.
5. Jacobi D, Liu S, Burkewitz K, Kory N, Knudsen Nelson H, Alexander Ryan K, et al. Hepatic Bmal1 Regulates Rhythmic Mitochondrial Dynamics and Promotes Metabolic Fitness. Cell Metab. 2015;22(4):709–720.
6. Camacho-Pereira J, Tarrago MG, Chini CCS, Nin V, Escande C, Warner GM, et al. CD38 Dictates Age-Related NAD Decline and Mitochondrial Dysfunction through an SIRT3-Dependent Mechanism. Cell Metab. 2016;23(6):1127–1139.
7. Qiu X, Brown K, Hirschey MD, Verdin E, Chen D. Calorie restriction reduces oxidative stress by SIRT3-mediated SOD2 activation. Cell Metab. 2010;12(6):662–667.
8. Kumar R, Mohan N, Upadhyay AD, Singh AP, Sahu V, Dwivedi S, et al. Identification of serum sirtuins as novel noninvasive protein markers for frailty. Aging Cell. 2014;13(6):975–980.
9. Brown KD, Maqsood S, Huang JY, Pan Y, Harkcom W, Li W, et al. Activation of SIRT3 by the $NAD^+$ precursor nicotinamide riboside protects from noise-induced hearing loss. Cell Metab. 2014;20(6):1059–1068.
10. Cantó C, Houtkooper RH, Pirinen E, Youn DY, Oosterveer MH, Cen Y, et al. The NAD(+) precursor nicotinamide riboside enhances oxidative metabolism and protects against high-fat diet-induced obesity. Cell Metab. 2012;15(6):838–847.
11. Diguet N, Trammell SAJ, Tannous C, Deloux R, Piquereau J, Mougenot N, et al. Nicotinamide Riboside Preserves Cardiac Function in a Mouse Model of Dilated Cardiomyopathy. Circulation. 2018;137(21):2256–2273.
12. Ear PH, Chadda A, Gumusoglu SB, Schmidt MS, Vogeler S, Malicoat J, et al. Maternal Nicotinamide Riboside Enhances Postpartum Weight Loss, Juvenile Offspring Development, and Neurogenesis of Adult Offspring. Cell Rep. 2019;26(4):969–983.

13. Bae K, Jin X, Maywood ES, Hastings MH, Reppert SM, Weaver DR. Differential functions of mPer1, mPer2, and mPer3 in the SCN circadian clock. Neuron. 2001;30(2):525–536.
14. Shearman LP, Jin X, Lee C, Reppert SM, Weaver DR. Targeted Disruption of the mPer3 Gene: Subtle Effects on Circadian Clock Function. Mol Cell Biol. 2000;20(17):6269–6275.
15. Sheen MR, Fields JL, Northan B, Lacoste J, Ang LH, Fiering S. Replication Study: Biomechanical remodeling of the microenvironment by stromal caveolin-1 favors tumor invasion and metastasis. eLife. 2019;8:e45120.
16. Dang F, Sun X, Ma X, Wu R, Zhang D, Chen Y, et al. Insulin post-transcriptionally modulates Bmal1 protein to affect the hepatic circadian clock. Nat Commun. 2016;7(1):1–12.
17. Smeitink JA, Zeviani M, Turnbull DM, Jacobs HT. Mitochondrial medicine: A metabolic perspective on the pathology of oxidative phosphorylation disorders. Cell Metab. 2006;3(1):9–13.
18. Chen M, Chen Z, Wang Y, Tan Z, Zhu C, Li Y, et al. Mitophagy receptor FUNDC1 regulates mitochondrial dynamics and mitophagy. Autophagy. 2016;12(4):689–702.
19. Gao M, Yi J, Zhu J, Minikes AM, Monian P, Thompson CB, et al. Role of Mitochondria in Ferroptosis. Mol Cell. 2019;73(2):354–363.
20. Ramsey KM, Yoshino J, Brace CS, Abrassart D, Kobayashi Y, Marcheva B, et al. Circadian Clock Feedback Cycle Through NAMPT-Mediated $NAD^+$ Biosynthesis. Science. 2009;324(5927):651–654.
21. Nakahata Y, Sahar S, Astarita G, Kaluzova M, Sassone-Corsi P. Circadian control of the NAD + salvage pathway by CLOCK-SIRT1. Science. 2009;324(5927):654–657.
22. Imai S-i, Guarente L. $NAD^+$ and sirtuins in aging and disease. Trends Cell Biol. 2014;24(8):464–471.
23. Yang H, Yang T, Baur JA, Perez E, Matsui T, Carmona JJ, et al. Nutrient-sensitive mitochondrial $NAD^+$ levels dictate cell survival. Cell. 2007;130(6):1095–1107.
24. Pillai VB, Samant S, Sundaresan NR, Raghuraman H, Kim G, Bonner MY, et al. Honokiol blocks and reverses cardiac hypertrophy in mice by activating mitochondrial Sirt3. Nat Commun. 2015;6(1):1–16.
25. Darlington TK, Wager-Smith K, Ceriani MF, Staknis D, Gekakis N, Steeves TD, et al. Closing the circadian loop: CLOCK-induced transcription of its own inhibitors per and tim. Science. 1998;280(5369):1599–1603.
26. Aggarwal A, Costa MJ, Rivero-Gutiérrez B, Ji L, Morgan SL, Feldman BJ. The Circadian Clock Regulates Adipogenesis by a Per3 Crosstalk Pathway to Klf15. Cell Rep. 2017;21(9):2367–2375.
27. Costa MJ, So AY, Kaasik K, Krueger KC, Pillsbury ML, Fu YH, et al. Circadian rhythm gene period 3 is an inhibitor of the adipocyte cell fate. J Biol Chem. 2011;286(11):9063–9070.
28. Zhang L, Hirano A, Hsu PK, Jones CR, Sakai N, Okuro M, et al. A PERIOD3 variant causes a circadian phenotype and is associated with a seasonal mood trait. Proc Natl Acad Sci USA. 2016;113(11):1536–1544.
29. Boutant M, Kulkarni SS, Joffraud M, Ratajczak J, Valera-Alberni M, Combe R, et al. Mfn2 is critical for brown adipose tissue thermogenic function. Embo J. 2017;36(11):1543–1558.

30. Song M, Dorn Gerald W. Mitoconfusion: Noncanonical Functioning of Dynamism Factors in Static Mitochondria of the Heart. Cell Metab. 2015;21(2):195–205.
31. Schmitt K, Grimm A, Dallmann R, Oettinghaus B, Restelli LM, Witzig M, et al. Circadian Control of DRP1 Activity Regulates Mitochondrial Dynamics and Bioenergetics. Cell Metab. 2018;27(3):657–666.
32. Balaban RS, Nemoto S, Finkel T. Mitochondria, oxidants, and aging. Cell. 2005;120(4):483–495.
33. Wallace DC. A mitochondrial paradigm of metabolic and degenerative diseases, aging, and cancer: a dawn for evolutionary medicine. Annu Rev Genet 2005;39(1): 359–407.
34. Wallace DC, Fan W. The pathophysiology of mitochondrial disease as modeled in the mouse. Genes Dev. 2009;23(15):1714–1736.
35. Zhou ZD, Tan EK. Oxidized nicotinamide adenine dinucleotide-dependent mitochondrial deacetylase sirtuin-3 as a potential therapeutic target of Parkinson's disease. Ageing Res Rev. 2020;62(1):101107.
36. Klimova N, Long A, Kristian T. Nicotinamide mononucleotide alters mitochondrial dynamics by SIRT3-dependent mechanism in male mice. J Neurosci Res. 2019;97(8):975–990.
37. Xie X, Shu R, Yu C, Fu Z, Li Z. Mammalian AKT, the Emerging Roles on Mitochondrial Function in Diseases. Aging Dis. 2022;13(1):157–174.
38. Amano H, Chaudhury A, Rodriguez-Aguayo C, Lu L, Akhanov V, Catic A, et al. Telomere Dysfunction Induces Sirtuin Repression that Drives Telomere-Dependent Disease. Cell Metab. 2019;29(6):1274–1290.
39. Mitchell SJ, Bernier M, Aon MA, Cortassa S, Kim EY, Fang EF, et al. Nicotinamide Improves Aspects of Healthspan, but Not Lifespan, in Mice. Cell Metab. 2018;27(3):667–676.
40. Mouchiroud L, Houtkooper RH, Moullan N, Katsyuba E, Ryu D, Cantó C, et al. The NAD(+)/Sirtuin Pathway Modulates Longevity through Activation of Mitochondrial UPR and FOXO Signaling. Cell. 2013;154(2):430–441.
41. Gardell SJ, Hopf M, Khan A, Dispagna M, Hampton Sessions E, Falter R, et al. Boosting $NAD^{(+)}$ with a small molecule that activates NAMPT. Nat Commun. 2019;10(1):3241.
42. Hor J-H, Santosa MM, Lim VJW, Ho BX, Taylor A, Khong ZJ, et al. ALS motor neurons exhibit hallmark metabolic defects that are rescued by SIRT3 activation. Cell Death Differ. 2021;28(4):1379–1397.
43. Lee JJ, van de Ven RAH, Zaganjor E, Ng MR, Barakat A, Demmers J, et al. Inhibition of epithelial cell migration and Src/FAK signaling by SIRT3. Proc Natl Acad Sci USA. 2018;115(27):7057–7062.

# Figures

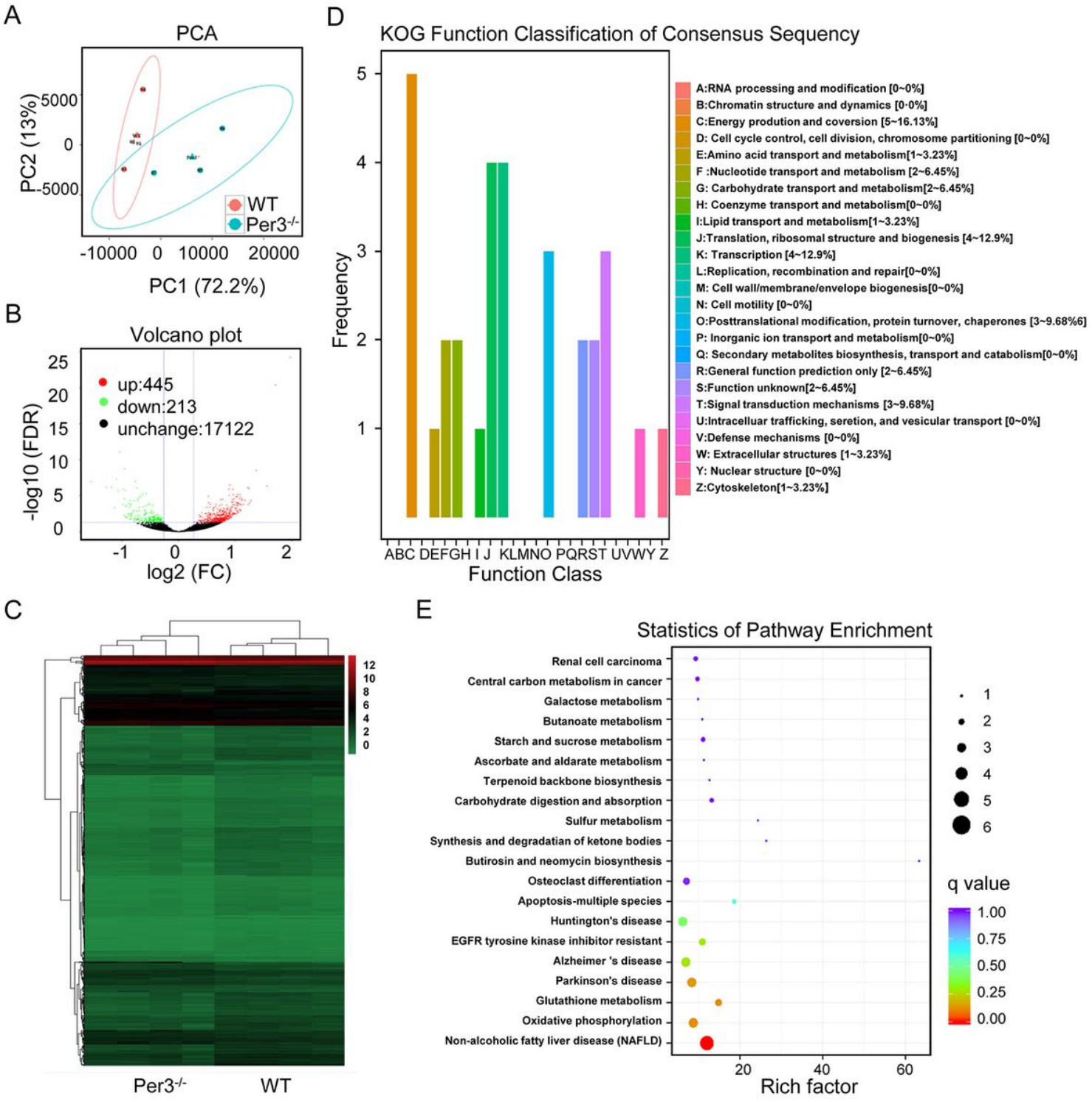


## Figure 1

Loss of PER3 affects cellular energy status in the liver. (**A-E**) Gene expression analysis in the liver tissues of wild-type (WT) and *Per3* deficient mice. (**A**) PCA analysis, (**B, C**) Volcano plots (**B**) and heat map (**C**) of differentially expressed genes. (**D**) Orthologous group analysis. (**E**) KEGG pathway enrichment analysis. Values represent the mean ± SEM (n=8 mice/group). $^{*}p<0.05$, $^{**}p<0.01$ vs. WT mice.

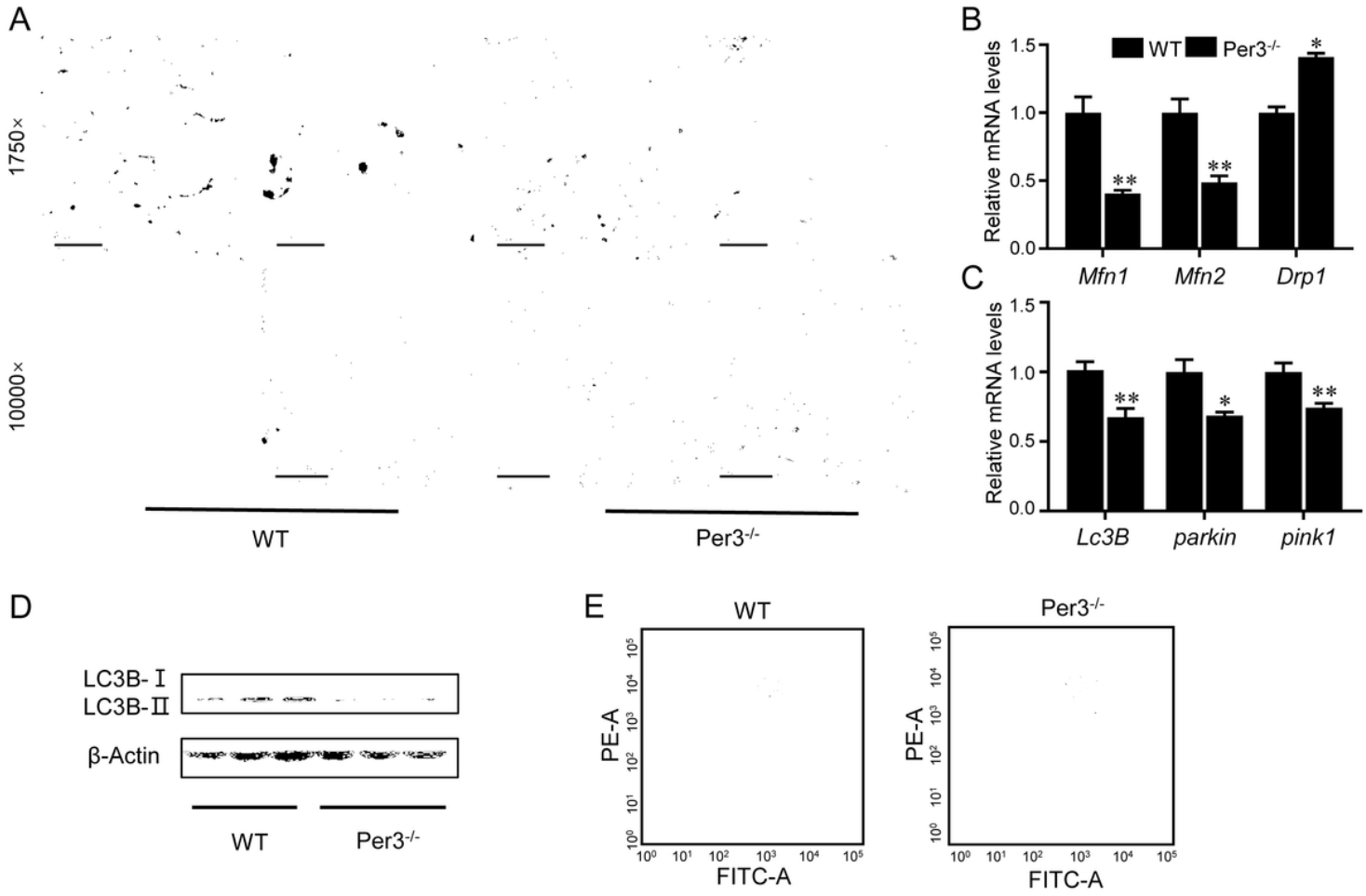


## Figure 2

Loss of PER3 disrupts mitochondrial homeostasis and energy metabolism.

(**A**) PER3 depletion affects the mitochondrial morphology screened by TEM. (**B**) Effect of PER3 deficiency on mRNA expressions of *Mfn1*, *Mfn2*, and *Drp1*. (**C, D**) *PER3* modulates autophagy-related mRNA expressions of *Lc3B*, *Parkin*, and *Pink1*, and protein expression of LC3B-I, LC3B-II in mice. (**E**) The effect of *Per3* knockout on modulation of mitochondrial membrane potential. Values represent the mean ± SEM (n = 8 /group). $^{*}p<0.05$, $^{**}p<0.01$ vs. WT mice.

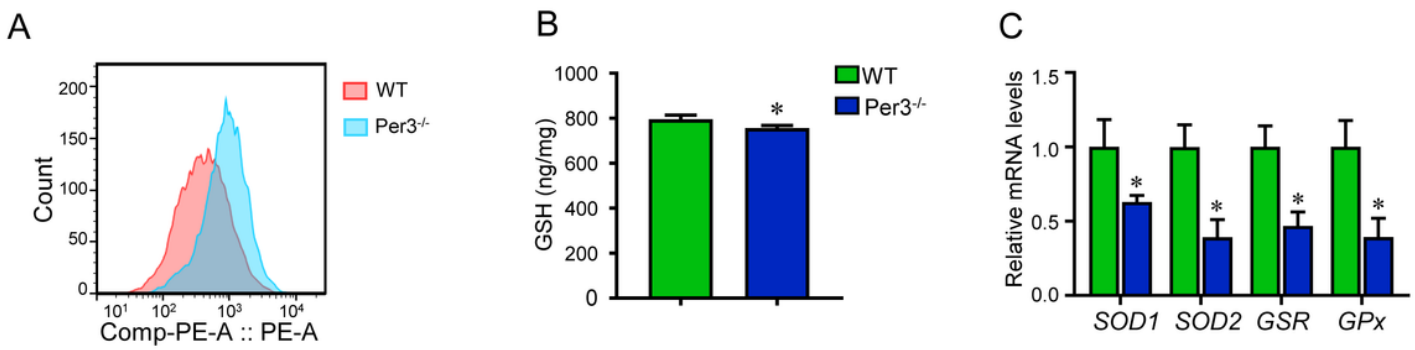


## Figure 3

PER3 depletion induces cellular oxidative stress in the liver. (**A**) Effects of PER3 loss on ROS generation. (**B**) GSH content. (**C**) Effect of *PER3* deficiency on mRNA expressions of *SOD1*, *SOD2*, *GSR*, and *GPx*. Values represent the mean ± SEM (n=8/group). $^{*}p<0.05$, $^{**}p<0.01$ vs. WT mice.

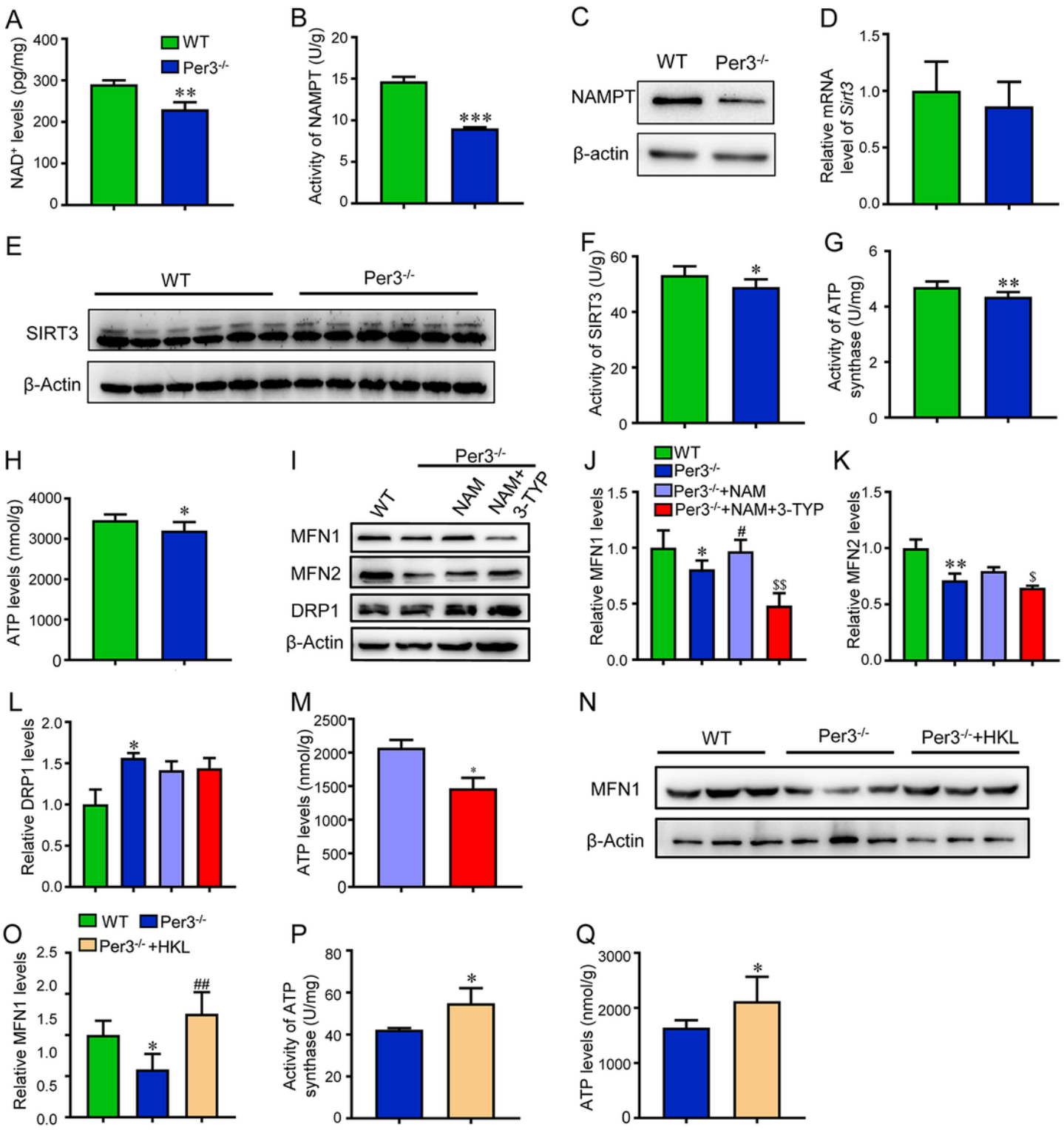


## Figure 4

PER3 controls mitochondrial homeostasis via the NAD$^+$-SIRT3 axis. (**A**) NAD$^+$ levels. (**B**) NAMPT activity. (**C**) level of NAMPT protein. (**D, E**) mRNA and protein expressions of Sirt3. (**F**) SIRT3 activity. (**G**) ATP synthase activity. (**H**) Analysis of ATP levels in Per3 deficient mice. (**I**) Protein levels of MFN1, MFN2, and DRP1 were analyzed by western blotting. (**J-L**) Quantification of MFN1, MFN2, and DRP1 protein levels. (**M**) 3-TYP abolished the effects of NAM on ATP production. Honokiol (HKL) rescued the effects of Per3

depletion on (**N-O**) MFN1 levels, (**P**) ATP levels, (**Q**) ATP synthase activity. Values represent the mean ± SEM (n=8/group). $^{*}p<0.05$, $^{**}p<0.01$ vs. controls.

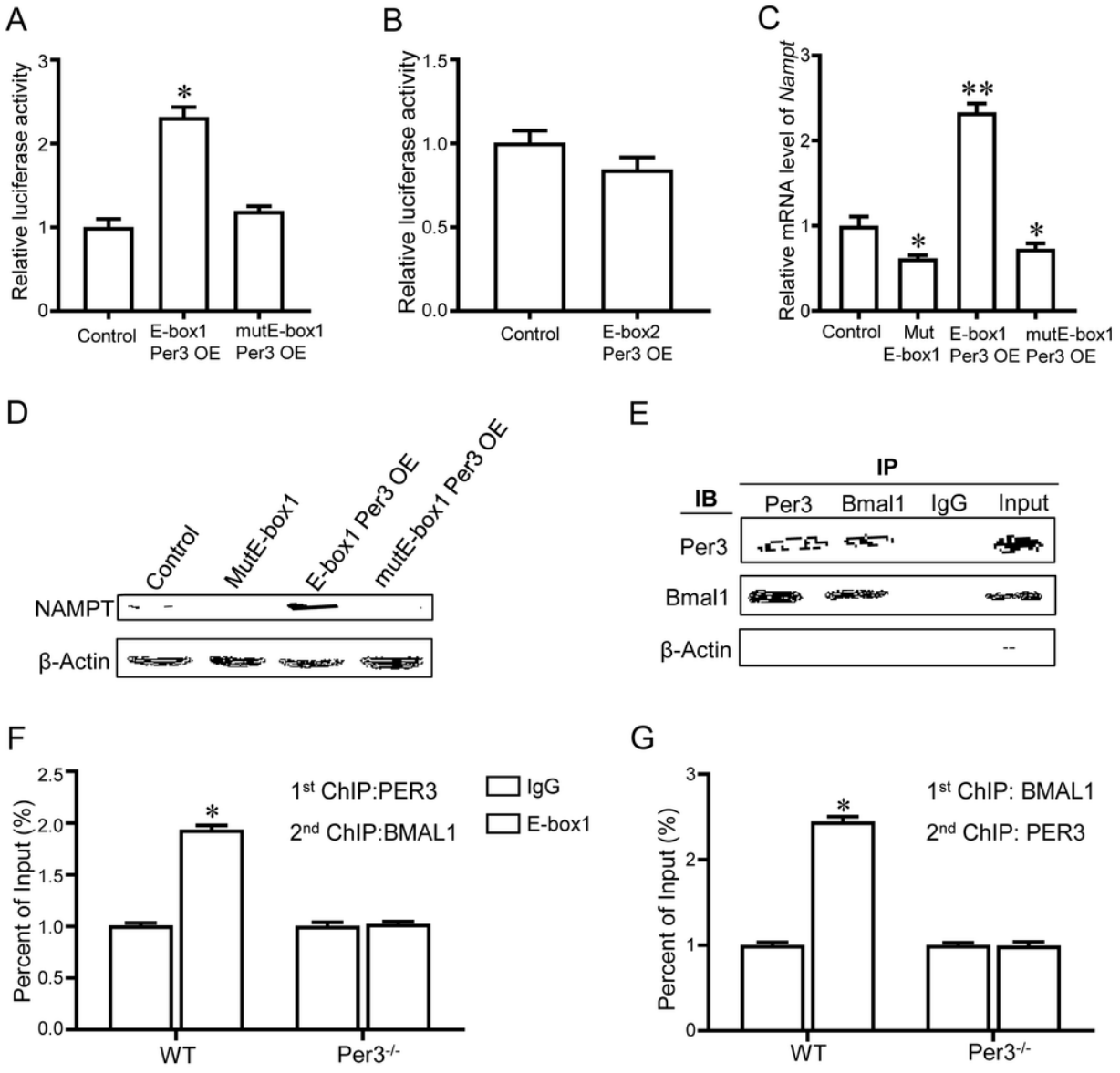


## Figure 5

The expression of *NAMPT* is directly modulated by PER3 and BMAL1.

(**A**) Luciferase assay in HEK293T cells transfected with reporter plasmids containing *NAMPT* WT E-box1 or reporter plasmid with E-box1 mutated sequence co-transfected with PER3 overexpression plasmid. (**B**) Luciferase assay in HEK293T cells transfected with reporter plasmids containing *NAMPT* WT E-box2 co-transfected with PER3 overexpression plasmid. (**C-D**) Effects of E-box1 mutation and PER3 overexpression on NAMPT mRNA and protein expression. (**E**) The co-IP assay was performed using anti-BMAL1, and anti-PER3 antibodies. (**F-G**) ChIP analysis using antibodies against PER3, BMAL1, or IgG

control at E-box1 site of *Nampt* gene in PMEFs isolated from WT and *Per3* KO mice. Values represent the mean ± SEM (n=8/group). $^{*}p<0.05$, $^{**}p<0.01$ vs. controls.

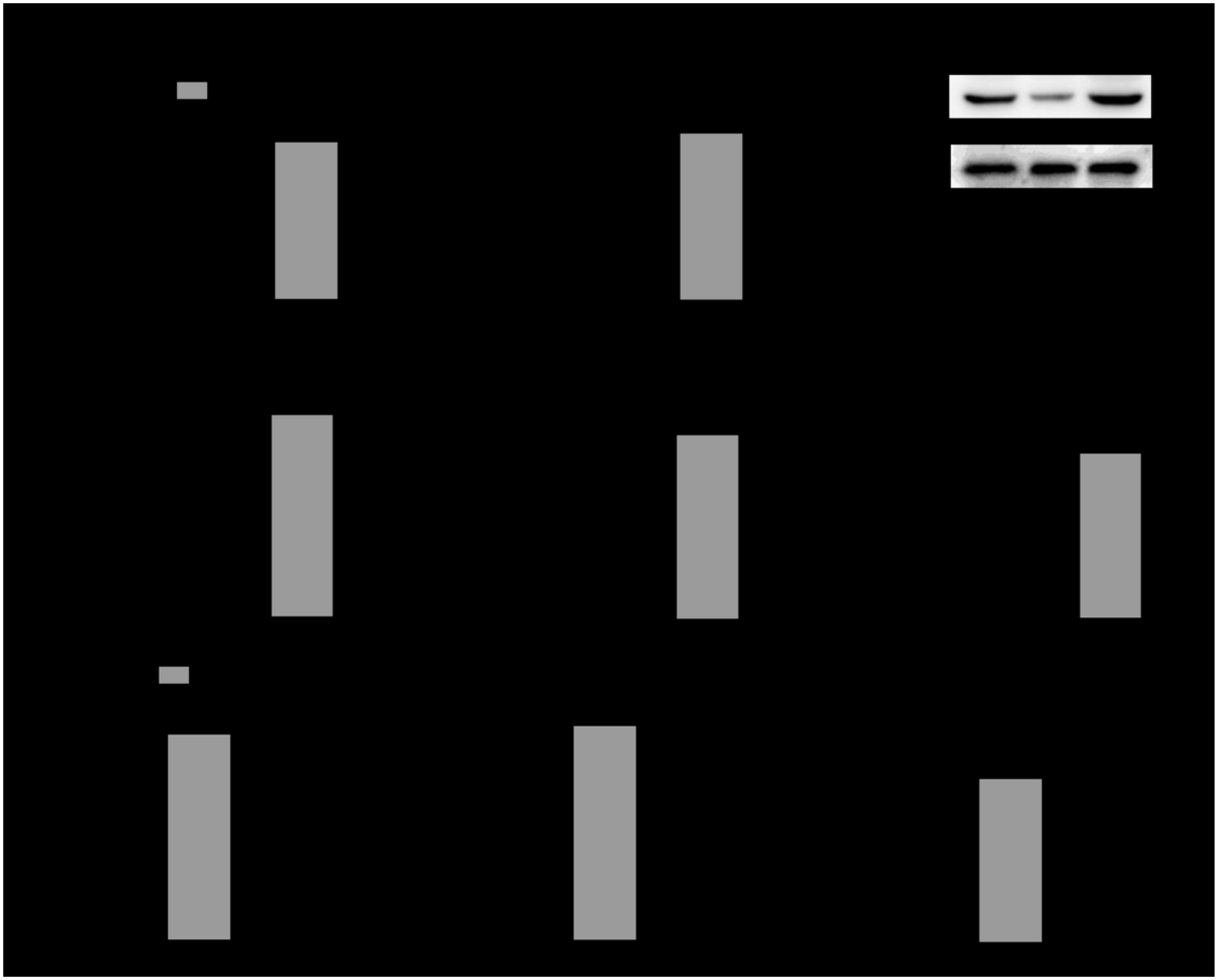

**Figure 6**

NAM mitigates *Per3* deletion-induced mitochondrial energy deficiency. NAM treatment rescued the pathological effects of Per3 depletion on (**A**) $NAD^+$ levels, (**B, C**) NAMPT activity and its protein level, (**D**) SIRT3 activity, (**E**) ATP synthase activity, and (**F**) ATP levels. In PMEFs, 3-TYP exposure suppressed the effects of NAM administration on (**G**) SIRT3 activity, (**H**) ATP synthase activity, and (**I**) $NAD^+$ levels. Values represent the mean ± SEM (n=8/group). $^{*}p<0.05$, $^{**}p<0.01$ vs. controls.

# Supplementary Files

This is a list of supplementary files associated with this preprint. Click to download.

- FigS1.tif
- FigS2.tif
- SupplementaryTable1.docx
- graphicalfigure.tif
- OriginalfulllengthwesternblotsforPer3relatedmitochondria.pdf